

Non-Gaussian cumulants of conserved charge fluctuations

Sayantana Sharma



Project Members: Frithjof Karsch, Swagato Mukherjee, Hiroshi Ohno, Peter Petreczky and Patrick Steinbrecher

USQCD All Hands Meeting 2016.

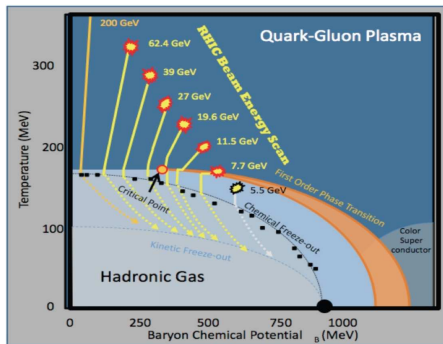
Outline

- 1 Goals of our project
- 2 Recent developments
- 3 New Results and Outlook

Outline

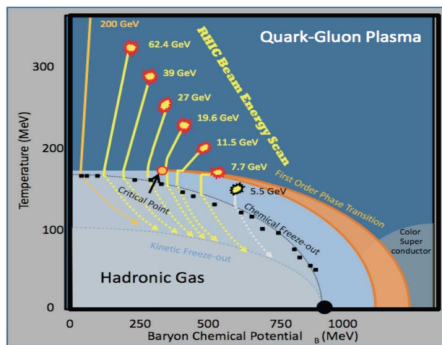
- 1 Goals of our project
- 2 Recent developments
- 3 New Results and Outlook

QCD Phase Diagram: Status



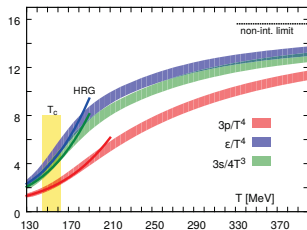
- QCD phase diagram largely unexplored inspite of intense efforts in last decades. → major focus of the Beam Energy Scan phase II experiments planned at the Relativistic Heavy Ion Collider at BNL.

QCD Phase Diagram: Status



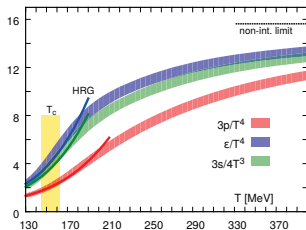
- QCD phase diagram largely unexplored inspite of intense efforts in last decades. → major focus of the Beam Energy Scan phase II experiments planned at the Relativistic Heavy Ion Collider at BNL.
- Themes: Existence of critical end-point, hydrodynamic modeling of the QCD medium formed in the experiments to understand experimental results.

Goals of our project



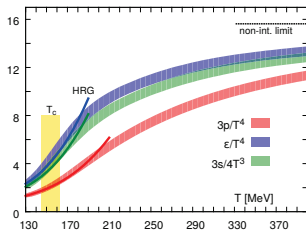
- Lattice studies have given an Equation of state in QCD at $\mu_B = 0$ in the continuum limit. [HotQCD and Budapest-Wuppertal Collaboration]
- $T \sim 140$ MeV, QCD can be described as Hadron Resonance Gas model but near chiral crossover $T_c \sim 154$ MeV, HRG picture breaks down.

Goals of our project



- Lattice studies have given an Equation of state in QCD at $\mu_B = 0$ in the continuum limit. [HotQCD and Budapest-Wuppertal Collaboration]
 - $T \sim 140$ MeV, QCD can be described as Hadron Resonance Gas model but near chiral crossover $T_c \sim 154$ MeV, HRG picture breaks down.
-
- What happens to the HRG picture at finite density like the QCD medium formed in the experiments?

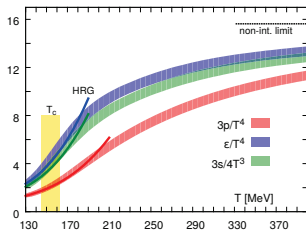
Goals of our project



- Lattice studies have given an Equation of state in QCD at $\mu_B = 0$ in the continuum limit. [HotQCD and Budapest-Wuppertal Collaboration]
- $T \sim 140$ MeV, QCD can be described as Hadron Resonance Gas model but near chiral crossover $T_c \sim 154$ MeV, HRG picture breaks down.

- What happens to the HRG picture at finite density like the QCD medium formed in the experiments?
- Can we bracket the position of the critical end-point in QCD phase diagram?

Goals of our project



- Lattice studies have given an Equation of state in QCD at $\mu_B = 0$ in the continuum limit. [HotQCD and Budapest-Wuppertal Collaboration]
- $T \sim 140$ MeV, QCD can be described as Hadron Resonance Gas model but near chiral crossover $T_c \sim 154$ MeV, HRG picture breaks down.

- What happens to the HRG picture at finite density like the QCD medium formed in the experiments?
- Can we bracket the position of the critical end-point in QCD phase diagram?
- Can we understand the critical behaviour due to the light quarks in the crossover region?

Critical point: status

- One of the methods to circumvent **sign problem** at finite μ :
Taylor expansion of physical observables around $\mu = 0$ in powers of μ/T .

Critical point: status

- One of the methods to circumvent **sign problem** at finite μ :
Taylor expansion of physical observables around $\mu = 0$ in powers of μ/T .

- The baryon no. susceptibility:

$$\chi_2^B(\mu_B)/T^2 = \chi_2^B(0)/T^2 + \frac{1}{2} \left(\frac{\mu_B}{T}\right)^2 \chi_4^B(0) + \frac{1}{4!} \left(\frac{\mu_B}{T}\right)^4 \chi_6^B(0) + \dots$$

Critical point: status

- One of the methods to circumvent **sign problem** at finite μ :
Taylor expansion of physical observables around $\mu = 0$ in powers of μ/T .
- The baryon no. susceptibility:
$$\chi_2^B(\mu_B)/T^2 = \chi_2^B(0)/T^2 + \frac{1}{2} \left(\frac{\mu_B}{T}\right)^2 \chi_4^B(0) + \frac{1}{4!} \left(\frac{\mu_B}{T}\right)^4 \chi_6^B(0) + \dots$$
- Series should diverge at the critical point. On finite lattice χ_2^B peaks, ratios of Taylor coefficients equal, indep. of volume [Gavai& Gupta, 03]

Critical point: status

- One of the methods to circumvent **sign problem** at finite μ :
Taylor expansion of physical observables around $\mu = 0$ in powers of μ/T .
- The baryon no. susceptibility:
$$\chi_2^B(\mu_B)/T^2 = \chi_2^B(0)/T^2 + \frac{1}{2} \left(\frac{\mu_B}{T}\right)^2 \chi_4^B(0) + \frac{1}{4!} \left(\frac{\mu_B}{T}\right)^4 \chi_6^B(0) + \dots$$
- Series should diverge at the critical point. On finite lattice χ_2^B peaks, ratios of Taylor coefficients equal, indep. of volume [Gavai & Gupta, 03]
- Current status:
 χ_8^B for $N_\tau = 8$ pure staggered fermions [Gavai & Gupta, 08].
 χ_6^B for $N_\tau = 6, 8, 12, 16$ HISQ fermions
[BNL-Bielefeld-CCNU Collaboration, HotQCD Collaboration, 16].

Critical point: status

- One of the methods to circumvent **sign problem** at finite μ :
Taylor expansion of physical observables around $\mu = 0$ in powers of μ/T .
- The baryon no. susceptibility:
$$\chi_2^B(\mu_B)/T^2 = \chi_2^B(0)/T^2 + \frac{1}{2} \left(\frac{\mu_B}{T}\right)^2 \chi_4^B(0) + \frac{1}{4!} \left(\frac{\mu_B}{T}\right)^4 \chi_6^B(0) + \dots$$
- Series should diverge at the critical point. On finite lattice χ_2^B peaks, ratios of Taylor coefficients equal, indep. of volume [Gavai & Gupta, 03]
- Current status:
 χ_8^B for $N_\tau = 8$ pure staggered fermions [Gavai & Gupta, 08].
 χ_6^B for $N_\tau = 6, 8, 12, 16$ HISQ fermions
[BNL-Bielefeld-CCNU Collaboration, HotQCD Collaboration, 16].
- χ_6^B can already constrain QCD pressure in the regime approximated by Hadron Resonance gas model.

Challenges

- The Baryon no. susceptibilities can be expressed in terms of Quark no. susceptibilities (QNS).

Challenges

- The Baryon no. susceptibilities can be expressed in terms of Quark no. susceptibilities (QNS).
- QNS χ_{ij} 's can be written as derivatives of the Dirac operator.
Example : $\chi_2^u = \frac{T}{V} \langle \text{Tr}(D_u^{-1} D_u'' - (D_u^{-1} D_u')^2) + (\text{Tr}(D_u^{-1} D_u'))^2 \rangle$.
 $\chi_{11}^{us} = \frac{T}{V} \langle \text{Tr}(D_u^{-1} D_u' D_s^{-1} D_s') \rangle$.

Challenges

- The Baryon no. susceptibilities can be expressed in terms of Quark no. susceptibilities (QNS).
- QNS χ_{ij} 's can be written as derivatives of the Dirac operator.
Example : $\chi_2^u = \frac{T}{V} \langle \text{Tr}(D_u^{-1} D_u'' - (D_u^{-1} D_u')^2) + (\text{Tr}(D_u^{-1} D_u'))^2 \rangle$.
 $\chi_{11}^{us} = \frac{T}{V} \langle \text{Tr}(D_u^{-1} D_u' D_s^{-1} D_s') \rangle$.
- Inversions performed on Gaussian noise vectors

Challenges

- The Baryon no. susceptibilities can be expressed in terms of Quark no. susceptibilities (QNS).
- QNS χ_{ij} 's can be written as derivatives of the Dirac operator.
Example : $\chi_2^u = \frac{T}{V} \langle \text{Tr}(D_u^{-1} D_u'' - (D_u^{-1} D_u')^2) + (\text{Tr}(D_u^{-1} D_u'))^2 \rangle$.
 $\chi_{11}^{us} = \frac{T}{V} \langle \text{Tr}(D_u^{-1} D_u' D_s^{-1} D_s') \rangle$.
- Inversions performed on Gaussian noise vectors
- Higher derivatives \rightarrow more inversions
Inversion is the most expensive step on the lattice !

Challenges

- The Baryon no. susceptibilities can be expressed in terms of Quark no. susceptibilities (QNS).
- QNS χ_{ij} 's can be written as derivatives of the Dirac operator.
Example : $\chi_2^u = \frac{T}{V} \langle \text{Tr}(D_u^{-1} D_u'' - (D_u^{-1} D_u')^2) + (\text{Tr}(D_u^{-1} D_u'))^2 \rangle$.
 $\chi_{11}^{us} = \frac{T}{V} \langle \text{Tr}(D_u^{-1} D_u' D_s^{-1} D_s') \rangle$.
- Inversions performed on Gaussian noise vectors
- Higher derivatives \rightarrow more inversions
Inversion is the most expensive step on the lattice !
- Extending to higher orders?

Challenges

- The Baryon no. susceptibilities can be expressed in terms of Quark no. susceptibilities (QNS).
- QNS χ_{ij} 's can be written as derivatives of the Dirac operator.
Example : $\chi_2^u = \frac{T}{V} \langle \text{Tr}(D_u^{-1} D_u'' - (D_u^{-1} D_u')^2) + (\text{Tr}(D_u^{-1} D_u'))^2 \rangle$.
 $\chi_{11}^{us} = \frac{T}{V} \langle \text{Tr}(D_u^{-1} D_u' D_s^{-1} D_s') \rangle$.
- Inversions performed on Gaussian noise vectors
- Higher derivatives \rightarrow more inversions
Inversion is the most expensive step on the lattice !
- Extending to higher orders?
 - 1 Matrix inversions increasing with the order

Challenges

- The Baryon no. susceptibilities can be expressed in terms of Quark no. susceptibilities (QNS).
- QNS χ_{ij} 's can be written as derivatives of the Dirac operator.
Example : $\chi_2^u = \frac{T}{V} \langle \text{Tr}(D_u^{-1} D_u'' - (D_u^{-1} D_u')^2) + (\text{Tr}(D_u^{-1} D_u'))^2 \rangle$.
 $\chi_{11}^{us} = \frac{T}{V} \langle \text{Tr}(D_u^{-1} D_u' D_s^{-1} D_s') \rangle$.
- Inversions performed on Gaussian noise vectors
- Higher derivatives \rightarrow more inversions
Inversion is the most expensive step on the lattice !
- Extending to higher orders?
 - 1 Matrix inversions increasing with the order
 - 2 Delicate cancellation between a large number of terms for higher order QNS.

Outline

- 1 Goals of our project
- 2 Recent developments
- 3 New Results and Outlook

A new method to introduce μ

- The staggered fermion matrix used at finite μ [Hasenfratz, Karsch ,83]

$$D(\mu)_{xy} = \sum_{i=1}^3 \eta_i(x) \left[U_i^\dagger(y) \delta_{x,y+\hat{i}} - U_i(x) \delta_{x,y-\hat{i}} \right] \\ + \eta_4(x) \left[e^{\mu a} U_4^\dagger(y) \delta_{x,y+\hat{4}} - e^{-\mu a} U_4(x) \delta_{x,y-\hat{4}} \right]$$

A new method to introduce μ

- The staggered fermion matrix used at finite μ [Hasenfratz, Karsch ,83]

$$D(\mu)_{xy} = \sum_{i=1}^3 \eta_i(x) \left[U_i^\dagger(y) \delta_{x,y+\hat{i}} - U_i(x) \delta_{x,y-\hat{i}} \right] \\ + \eta_4(x) \left[e^{\mu a} U_4^\dagger(y) \delta_{x,y+\hat{4}} - e^{-\mu a} U_4(x) \delta_{x,y-\hat{4}} \right]$$

- One can also add μ coupled to the conserved number density as in the continuum.

$$D(0)_{xy} - \frac{\mu a}{2} \eta_4(x) \left[U_4^\dagger(y) \delta_{x,y+\hat{4}} + U_4(x) \delta_{x,y-\hat{4}} \right] .$$

Pros and Cons

- Linear method: $D' = \sum_{x,y} N(x,y)$, and
 $D'' = D''' = D'''' \dots = 0$

in contrast to the Exp-prescription, all derivatives are non-zero.

Pros and Cons

- Linear method: $D' = \sum_{x,y} N(x,y)$, and
 $D'' = D''' = D'''' \dots = 0$

in contrast to the Exp-prescription, all derivatives are non-zero.

- No. of inversions significantly reduced for higher orders in linear method.

For 8th order QNS the no. of matrix inversions reduced from 20 to 8.

[Gavai & Sharma, 12]

Pros and Cons

- Linear method: $D' = \sum_{x,y} N(x,y)$, and
 $D'' = D''' = D'''' \dots = 0$

in contrast to the Exp-prescription, all derivatives are non-zero.

- No. of inversions significantly reduced for higher orders in linear method.

For 8th order QNS the no. of matrix inversions reduced from 20 to 8.

[Gavai & Sharma, 12]

- Linear method: χ_n have additional zero- T artifacts. \rightarrow explicit counter terms needed for $\chi_{2,4}$, discussed in detail [Gavai & Sharma, 15]

Pros and Cons

- Linear method: $D' = \sum_{x,y} N(x,y)$, and
 $D'' = D''' = D'''' \dots = 0$

in contrast to the Exp-prescription, all derivatives are non-zero.

- No. of inversions significantly reduced for higher orders in linear method.

For 8th order QNS the no. of matrix inversions reduced from 20 to 8.

[Gavai & Sharma, 12]

- Linear method: χ_n have additional zero- T artifacts. \rightarrow explicit counter terms needed for $\chi_{2,4}$, discussed in detail [Gavai & Sharma, 15]
- In Exp method: counter terms already at the Lagrangian level. We use this method for χ_n^B , $n = 2, 4$.

Nature of the divergences for higher order susceptibilities

- For any order n , the artifacts $\sim \mathcal{O}(a^{n-4})$.

Nature of the divergences for higher order susceptibilities

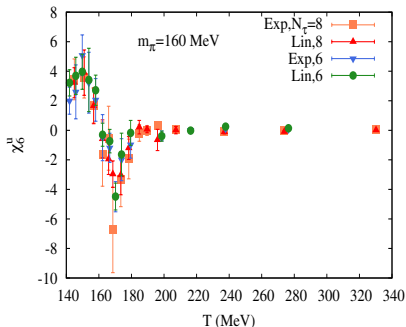
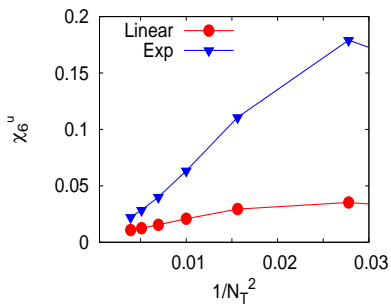
- For any order n , the artifacts $\sim \mathcal{O}(a^{n-4})$.
- $n \geq 6$ these artifacts do not affect the continuum extrapolation.

Nature of the divergences for higher order susceptibilities

- For any order n , the artifacts $\sim \mathcal{O}(a^{n-4})$.
- $n \geq 6$ these artifacts do not affect the continuum extrapolation.
- Explicitly checked in free theory as well as for QCD with HISQ fermions with nearly physical pion mass.

Nature of the divergences for higher order susceptibilities

- For any order n , the artifacts $\sim \mathcal{O}(a^{n-4})$.
- $n \geq 6$ these artifacts do not affect the continuum extrapolation.
- Explicitly checked in free theory as well as for QCD with HISQ fermions with nearly physical pion mass.

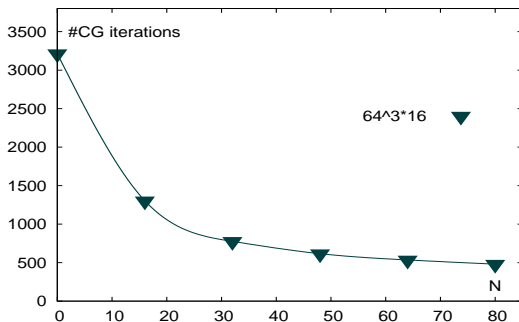


Speeding up the inversions with deflation

- Calculating explicitly the lowest eigenvalues improves performance of the fermion inverter

$$D^{-1}|R\rangle = \sum_{i=1}^N 1/\lambda_i |\psi_i\rangle \langle \psi_i | R \rangle + \text{CG Inversion.}$$

- We have developed highly optimized codes based on Ritz and Lanczos algorithms for CPU's and GPU respectively.
- Current volumes $N_s = 4N_\tau$, already approaches a plateau for $N = 80$ for $T \sim 145$ MeV. Typical $N = 192 - 256$.

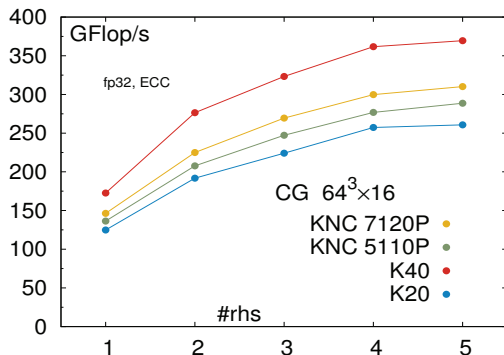


Performance of our codes

- We group random vectors for a single gauge configuration → use of **Multiple right hand sides** for Conjugate Gradient Inversion increases arithmetic intensity. [O. Kaczmarek, C. Schmidt, P. Steinbrecher, M. Wagner, 14]

Performance of our codes

- We group random vectors for a single gauge configuration → use of **Multiple right hand sides** for Conjugate Gradient Inversion increases arithmetic intensity. [O. Kaczmarek, C. Schmidt, P. Steinbrecher, M. Wagner, 14]
- Currently highly optimized codes for Intel Knights Corner extended to Knights Landing. [Mainly led by Patrick Steinbrecher, graduate student since 15]



Outline

- 1 Goals of our project
- 2 Recent developments
- 3 New Results and Outlook

New data analyzed 2015-16

T [MeV]	$32^3 \times 8$		$24^3 \times 6$	
	β	# analyzed	β	# analyzed
135	6.245	104420	5.980	68000
140	6.285	104480	6.015	120790
145	6.315	107480	6.045	120770
150	6.354	108030	6.080	30080
155	6.390	108580	6.120	23546
160	6.423	119290	6.150	31164
165	6.445	122340	6.170	20000
170	6.474	141780	6.200	138470
175	6.500	142960	6.225	125280

- Results with physical quark mass

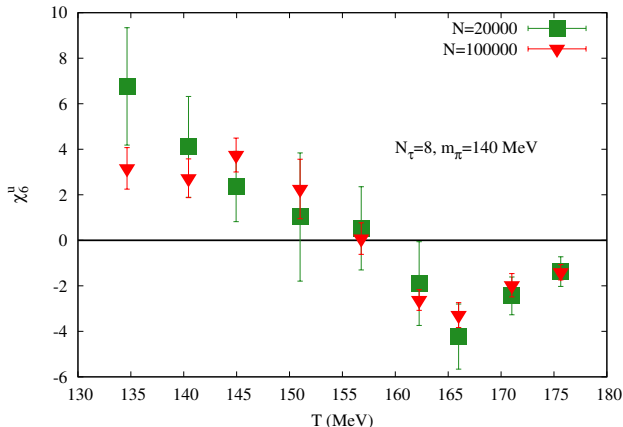
New data analyzed 2015-16

	$32^3 \times 8$		$24^3 \times 6$	
T [MeV]	β	# analyzed	β	# analyzed
135	6.245	104420	5.980	68000
140	6.285	104480	6.015	120790
145	6.315	107480	6.045	120770
150	6.354	108030	6.080	30080
155	6.390	108580	6.120	23546
160	6.423	119290	6.150	31164
165	6.445	122340	6.170	20000
170	6.474	141780	6.200	138470
175	6.500	142960	6.225	125280

- Results with physical quark mass
- Deflation + Multiple Right hand side technique+ special care of noisy operators \rightarrow a speedup of 30 allowed for analysis of extensive set of configurations.

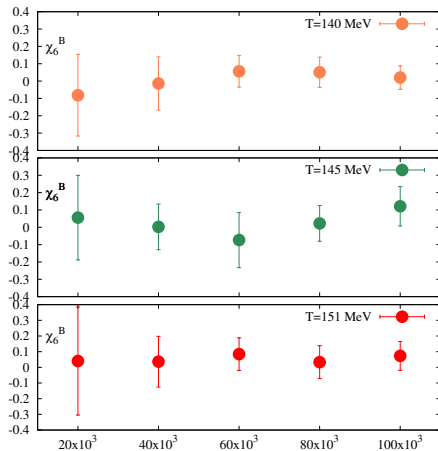
Main Outcome : Sixth order cumulants

- χ_6^u signal improved with the statistics N . We observe the negative dip just above $T_c \rightarrow$ signal of $O(4)$ criticality?



Main Outcome : Sixth order cumulants

- Improvement visible already in χ_6^B at the lowest temperatures by increasing number of configurations,
- We aim to increase statistics needed to reduce errors by a factor two.

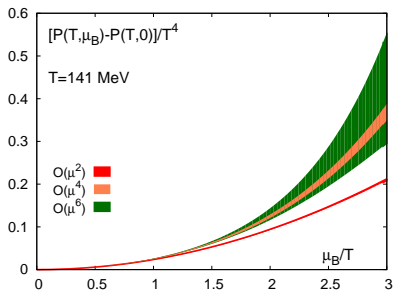
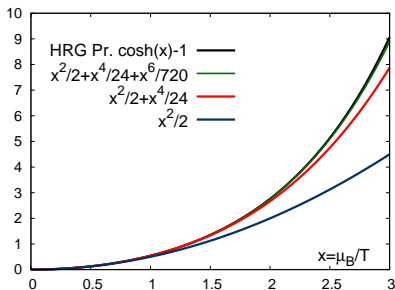


Constraining EoS

- In a regime where Hadron Resonance gas is anticipated to be a good description of QCD, including χ_6^B term already reproduces $P(\mu_B)$ within 5% accuracy.

Constraining EoS

- In a regime where Hadron Resonance gas is anticipated to be a good description of QCD, including χ_6^B term already reproduces $P(\mu_B)$ within 5% accuracy.
- Improve errors on our current data to observe this
→ increase statistics twofold this year.



Breakdown of HRG

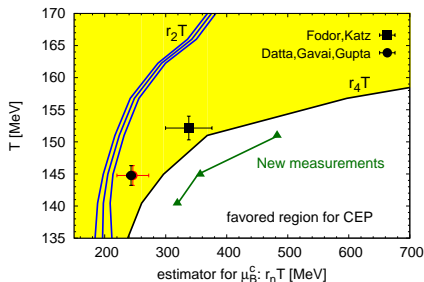
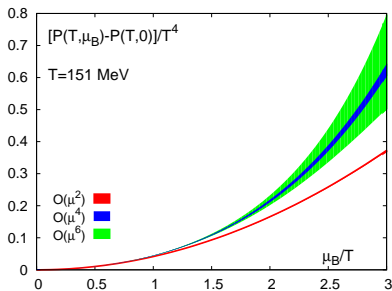
- Breakdown of HRG+ onset of criticality can be already constrained with χ_6^B .

Breakdown of HRG

- Breakdown of HRG+ onset of criticality can be already constrained with χ_6^B .
- Near critical point all terms in the Taylor expansion nearly equal \rightarrow need to improve the errors!

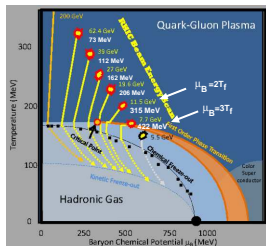
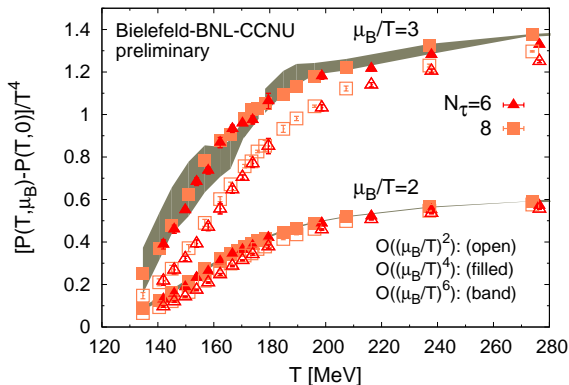
Breakdown of HRG

- Breakdown of HRG+ onset of criticality can be already constrained with χ_6^B .
- Near critical point all terms in the Taylor expansion nearly equal \rightarrow need to improve the errors!
- Our data gives a preliminary bound on the location of critical point from radius of convergence estimates, $r_{2n} \equiv \sqrt{2n(2n-1) \left| \frac{\chi_{2n}^B}{\chi_{2n+2}^B} \right|}$.

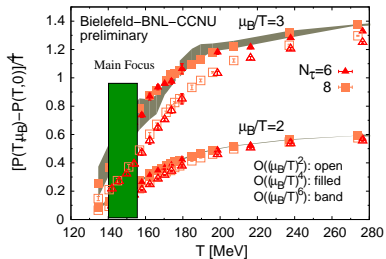


EoS away from criticality

- The pressure for $T > 160$ MeV which is an important input for the hydrodynamic modeling of the plasma already constrained by χ_B^6 even for highest μ_B/T .

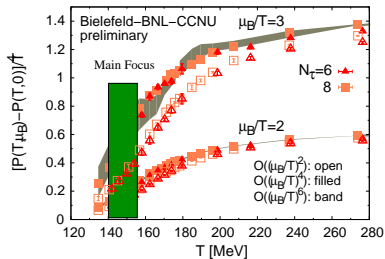


Outlook



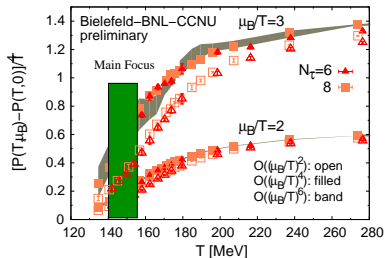
- In view of the RHIC Beam Energy Scan-II runs in 2019-20 it is important to have control over the Equation of State for $T \sim 145 - 160$ MeV.

Outlook



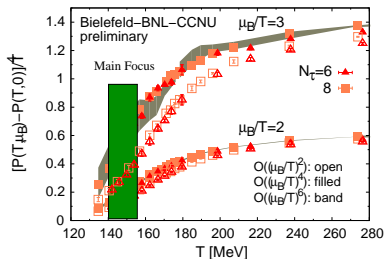
- In view of the RHIC Beam Energy Scan-II runs in 2019-20 it is important to have control over the Equation of State for $T \sim 145 - 160$ MeV.
- Improving statistics on χ_6^B in the hadron phase will already improve the EoS.

Outlook



- In view of the RHIC Beam Energy Scan-II runs in 2019-20 it is important to have control over the Equation of State for $T \sim 145 - 160$ MeV.
- Improving statistics on χ_6^B in the hadron phase will already improve the EoS.
- Analysis of χ_8^B is also crucial to estimate the errors on the EoS measured with the sixth order cumulants.

Outlook



- In view of the RHIC Beam Energy Scan-II runs in 2019-20 it is important to have control over the Equation of State for $T \sim 145 - 160$ MeV.
- Improving statistics on χ_6^B in the hadron phase will already improve the EoS.
- Analysis of χ_8^B is also crucial to estimate the errors on the EoS measured with the sixth order cumulants.
- Higher order cumulants will also help in bracketing the possible QCD critical end-point which is one of the focus of BES-II experiments.